Polarization behavior of femtosecond laser written optical waveguides in Ti:Sapphire

Jing Bai,[1,2] Guanghua Cheng,[1,*] Xuewen Long,[1,2] Yishan Wang,[1] Wei Zhao,[1] Guofu Chen,[1] Razvan Stoian,[3] and Rongqing Hui[4]

[1]*State Key Laboratory of Transient Optics and Photonics, Xi'an Institute of Optics and Precision Mechanics, Chinese Academy of Sciences, Xi'an 710119, China*

[2]*Graduate University of Chinese Academy of Sciences, Beijing, 100049, China*

[3]*Laboratoire Hubert Curien, UMR 5516 CNRS, Université de Lyon, Université Jean Monnet, 42000 Saint Etienne, France*

[4]*Department of Electrical Engineering and Computer Science, University of Kansas, Lawrence, Kansas 66044, USA*

[*]*gcheng@opt.ac.cn*

Abstract: Ultrashort pulsed laser photoinscription of Ti:Sapphire crystals may result in the self-organization of nanoscale material redistribution regions in regular patterns within the laser trace and stress-induced birefringence around the laser trace. We report on the formation of anisotropic optical waveguides in Ti:Sapphire by a procedure that involves femtosecond laser inscription of adjacent nonguiding birefringent traces with nanopatterned crosssections and the accumulation of stress birefringence in the region between. Double parallel line structures with a separation of 25μm with vertical and horizontal nanoscale arrangements were written with a choice of orthogonal polarizations. Due to anisotropic light scattering on periodic nanostructures and stress-induced birefringence in the central zone, remarkable polarization dependent guiding effects were observed as a function of the microscopic geometry of the structures. Building on this polarization sensitivity, several structure such as 3 × 3 waveguide arrays, diamond and hexagon patterns are also investigated.

OCIS codes: (140.3390) Laser materials processing; (130.5440) Polarization-selective devices. (050.6624) Subwavelength structures; (220.4000) Microstructure fabrication.

References and links

1. R. R. Thomson, S. Campbell, I. J. Blewett, A. K. Kar, and D. T. Reid, "Optical waveguide fabrication in z-cut lithium niobate ($LiNbO_3$) using femtosecond pulses in the low repetition rate regime," Appl. Phys. Lett. **88**(11), 111109 (2006).
2. J. Thomas, M. Heinrich, J. Burghoff, S. Nolte, A. Ancona, and A. Tüennermann, "Femtosecond laser-written quasi-phase-matched waveguides in lithium niobate," Appl. Phys. Lett. **91**(15), 151108 (2007).
3. Y. Shimotsuma, P. G. Kazansky, J. Qiu, and K. Hirao, "Self-organized nanogratings in glass irradiated by ultrashort light pulses," Phys. Rev. Lett. **91**(24), 247405 (2003).
4. V. R. Bhardwaj, E. Simova, P. P. Rajeev, C. Hnatovsky, R. S. Taylor, D. M. Rayner, and P. B. Corkum, "Optically produced arrays of planar nanostructures inside fused silica," Phys. Rev. Lett. **96**(5), 057404 (2006).
5. G. Cheng, K. Mishchik, C. Mauclair, E. Audouard, and R. Stoian, "Ultrafast laser photoinscription of polarization sensitive devices in bulk silica glass," Opt. Express **17**(12), 9515–9525 (2009).
6. J. Sipe, J. Young, J. Preston, and H. van Driel, "Laser-induced periodic surface structure. I. Theory," Phys. Rev. B **27**(2), 1141–1154 (1983).
7. R. Taylor, C. Hnatovsky, and E. Simova, "Applications of femtosecond laser induced self-organized planar nanocracks inside fused silica glass," Laser Photon. Rev. **2**(1-2), 26–46 (2008).
8. K. Mishchik, G. Cheng, G. Huo, I. M. Burakov, C. Mauclair, A. Mermillod-Blondin, A. Rosenfeld, Y. Ouerdane, A. Boukenter, O. Parriaux, and R. Stoian, "Nanosize structural modifications with polarization functions in ultrafast laser irradiated bulk fused silica," Opt. Express **18**(24), 24809–24824 (2010).
9. D. Wortmann, J. Gottmann, N. Brandt, and H. Horn-Solle, "Micro- and nanostructures inside sapphire by fs-laser irradiation and selective etching," Opt. Express **16**(3), 1517–1522 (2008).
10. V. Apostolopoulos, L. Laversenne, T. Colomb, C. Depeursinge, R. P. Salathé, M. Pollnau, R. Osellame, G. Cerullo, and P. Laporta, "Femtosecond-irradiation-induced refractive-index changes and channel waveguiding in bulk Ti^{3+}:Sapphire," Appl. Phys. Lett. **85**(7), 1122–1124 (2004).
11. J. Burghoff, S. Nolte, and A. Tünnermann, "Origins of waveguiding in femtosecond laser-structured LiNbO3," Appl. Phys., A Mater. Sci. Process. **89**(1), 127–132 (2007).

#166874 - $15.00 USD Received 17 Apr 2012; revised 25 May 2012; accepted 4 Jun 2012; published 20 Jun 2012

12. A. Szameit, D. Blömer, J. Burghoff, T. Pertsch, S. Nolte, and A. Tünnermann, "Hexagonal waveguide arrays written with fs-laser pulses," Appl. Phys. B **82**(4), 507–512 (2006).
13. A. Okhrimchuk, "Femtosecond fabrication of waveguides in ion-doped laser crystal," Coherence and Ultrashort Pulse Laser Emission, F. J. Duarte, ed., (InTech, 2010), pp. 519–542.
14. A. Mermillod-Blondin, I. M. Burakov, Y. P. Meshcheryakov, N. M. Bulgakova, E. Audouard, A. Rosenfeld, A. Husakou, I. V. Hertel, and R. Stoian, "Flipping the sign of refractive index changes in ultrafast and temporally shaped laser-irradiated borosilicate crown optical glass at high repetition rates," Phys. Rev. B **77**(10), 104205 (2008).
15. J. Morikawa, A. Orie, T. Hashimoto, and S. Juodkazis, "Thermal and optical properties of the femtosecond-laser-structured and stress-induced birefringent regions in sapphire," Opt. Express **18**(8), 8300–8310 (2010).
16. S. Juodkazis, K. Nishimura, S. Tanaka, H. Misawa, E. G. Gamaly, B. Luther-Davies, L. Hallo, P. Nicolai, and V. T. Tikhonchuk, "Laser-induced microexplosion confined in the bulk of a sapphire crystal: evidence of multimegabar pressures," Phys. Rev. Lett. **96**(16), 166101 (2006).
17. J. Sapriel, *Acousto-optics* (John Wiley and Sons, New York, 1979).
18. J. Xu and R. Stroud, *Acousto-optic Devices: Principles, Design, and Applications* (John Wiley and Sons, New York, 1992).
19. A. Couairon, L. Sudrie, M. Franco, B. Prade, and A. Mysyrowicz, "Filamentation and damage in fused silica induced by tightly focused femtosecond laser pulses," Phys. Rev. B **71**(12), 125435 (2005).
20. P. P. Rajeev, M. Gerstvolf, C. Hnatovsky, E. Simova, R. S. Taylor, P. B. Corkum, D. M. Rayner, and V. R. Bhardwaj, "Transient nanoplasmonics inside dielectrics," J. Phys. At. Mol. Opt. Phys. **40**(11), S273–S282 (2007).
21. M. Lancry, B. Poumellec, A. Chahid-Erraji, M. Beresna, and P. Kazansky, "Dependence of the femtosecond laser refractive index change thresholds on the chemical composition of doped-silica glasses," Opt. Mater. Express **1**(4), 711–723 (2011).
22. Y. Shimotsuma, K. Hirao, J. Qiu, and P. G. Kazansky, "Nano-modification inside transparent materials by femtosecond laser single beam," Mod. Phys. Lett. B **19**(5), 225–238 (2005).
23. T. Hashimoto, S. Juodkazis, and H. Misawa, "Void formation in glass," New J. Phys. **9**(8), 253 (2007).
24. M. Huang, "Stress effects on the performance of optical waveguides," Int. J. Solids Struct. **40**(7), 1615–1632 (2003).
25. V. Mizeikis, S. Kimura, N. Surovtsev, V. Jarutis, A. Saito, H. Misawa, and S. Juodkazis, "Formation of amorphous sapphire by a femtosecond laser pulse induced micro-explosion," Appl. Surf. Sci. **255**(24), 9745–9749 (2009).
26. S. Juodkazis, K. Nishimura, H. Misawa, T. Ebisui, R. Waki, S. Matsuo, and T. Okada, "Control over the Crystalline State of Sapphire," Adv. Mater. (Deerfield Beach Fla.) **18**(11), 1361–1364 (2006).

1. Introduction

Femtosecond (fs) direct laser writing (DLW) of transparent materials is a reliable and powerful micromachining technique emerged in the recent years. In such a way, a wide range of three-dimensional (3D) photonic devices manufactured using this method has been demonstrated in glasses and crystals [1,2]. When a femtosecond pulse is focused inside a dielectric material, the energy is only deposited in the vicinity of the focal spot due to a combination of nonlinear multi-photon absorption and avalanche ionization. If the deposited energy is sufficient, structural changes may occur in glasses, crystals and polymers, leading to a permanent modification in the dielectric function associated with a refractive index change. Above a certain irradiation dose and as a function of the material, a succession of dense and low density layers may appear, with subwavelength periodicities. In these processes, the laser electric field direction is a main factor in controlling both excitation efficiency and subsequent polarization of the dielectric matrix that assists the formation of ordered nanogratings. The resulting gratings in fused silica consist in narrow layers of lower index, oriented perpendicular to the laser electric field, with an interlayer period of approximately $\lambda/2n$, n being the refractive index and λ being the writing wavelength [3–5]. Similar nanogratings (although denoted as laser induced surface period structures, LIPSS) can be induced by polarized laser pulses on the surface of metals, semiconductors, and dielectrics [6]. The nanogratings formation with ultrashort laser pulses seems to be triggered essentially by electronic polarization effects as the molecular reorientation stays low during illumination. The dynamics of the nanogratings growth may involve collective electronic oscillations and local changes in polarizabilities which, due to a modulation of energy deposition and hydrodynamic matter redistribution, lead to the formation of a rippled structure under the condition of appropriate material relaxation.

#166874 - $15.00 USD Received 17 Apr 2012; revised 25 May 2012; accepted 4 Jun 2012; published 20 Jun 2012

All these phenomena may appear during fs waveguide writing and interesting characteristics of waveguides based on nanogratings have been observed: either morphologically under transmission scanning electrical microscopy (SEM) or optically in the guiding properties in e.g. fused silica [3]. A nanograting phenomenon leads to two main features; form birefringence with phase retardation and anisotropic scattering, namely polarization dependent scattering, with consequences in marking and phase control [7]. Polarization dependent scattering and resulting applications in light transport have been equally suggested [8]. Most cases concerning bulk nanogratings induced by fs laser pulses have been observed in fused silica and some derivates, rarely in other optical glasses or crystals, a situation that contrasts to surface ripples. A notable situation is the formation of nanostructures in bulk Ti:Sapphire, similar to the matrix material as reported by Wortmann et al. [9]. These regular nanopatterns can introduce certain polarization dependent guiding effects in Ti:Sapphire, putting forward a potential choice for fabricating polarizing elements in integrated photonic circuits. We note that, among the different solid state laser media, Ti:Sapphire is one of the most important materials as a laser medium due to its widely tunable output and broad absorption band. Especially, since it has a good thermo-conductivity, high optical damage threshold and allows high doping level of metal ions without significant degradation of spectroscopic characteristics, Ti:Sapphire crystal is a potential active media for fabrication of compact waveguide lasers. To this respect we point out that channel waveguides can be equally fabricated in Ti:Sapphire crystals by fs laser writing [10], an advantage to be considered in optical fabrication of embedded elements. Positive refractive-index changes necessary for waveguiding have been reported in the area above the tip of the damaged region induced by the laser pulse due to the redistribution of stress. Channel waveguides in particular are characterized by lower laser thresholds than bulk sapphire due to the guiding-mode confinement and excellent overlap between the laser mode and the pump. The combination of these effects, notably polarization and light guiding, may lead to an interesting set of optical functions and the development of 3D integrated photonic circuits.

However the fs inscribed waveguide in a crystal possesses new characteristics due to its anisotropy. Even though rarefaction or amorphization occur typically in the irradiated regions, positive index changes may appear at the extremity of the damage or be partially confined in between damage traces situated in close proximity due to stress accumulation and stress-induced birefringence. Firstly, in this case, the cladding of the waveguide may partially consist of the original crystal which is sensitive to the polarization. This leads to the possibility that the index of the cladding is smaller than the core induced by fs laser at some polarizations as the local birefringence may vary. Burghoff et al. [11] observed this kind of polarization dependent waveguiding in $LiNbO_3$ crystals, while similar structures in fused silica do not show a related polarization dependent guiding [12]. Secondly, we recall the formation of polarization sensitive nanopatterns within the confining traces.

Combining densification, nanograting formation, and stress-induced birefringence in the modified crystals, new optical functions can be predicted in sapphire crystals. In this article, we report on the fabrication of buried channel waveguides in Ti:Sapphire by using a double parallel line approach. Light confinement has been achieved between parallel micron-spaced tracks which posses nanostructured cross-sections. A remarkable polarization sensitivity of the guiding property was observed due to stress-induced polarization (accumulation of stress during photoinscription) in the interline region and the polarization dependent scattering properties of the nanostructures. The character of nanogratings in the sapphire crystal and possible formation mechanisms are discussed. Building on this basic geometry, the guiding of several 3D arrangements such as 3×3 waveguide arrays, diamond and hexagon structures are also investigated.

The paper is organized as follows. The experimental section describes the fabrication conditions and indicates the investigation details. The discussion part concentrates on two major issues. We firstly describe the structure and polarization dependent properties of the double track stress-confined waveguides in Ti:Sapphire in comparison to the $LiNbO_3$ crystals and fused silica, correlating the stressed refractive index change, core birefringence, and

#166874 - $15.00 USD Received 17 Apr 2012; revised 25 May 2012; accepted 4 Jun 2012; published 20 Jun 2012

optical scattering of the nanogratings. Secondly, we investigate the guiding properties of complex structure such as 3 × 3 waveguide arrays, diamond and hexagon arrangements.

2. Experimental setup

The schematic design of the experimental setup is shown in Fig. 1. A Ti:Sapphire CPA fs laser system (Spitfire, Spectra Physics) was used in the experiment. The central wavelength of the output laser pulses is 800 nm and the repetition rate is 1kHz The pulse duration was 120 fs. A shutter is used to control the irradiation time of the laser pulses in the sample. The pulse energy is controlled with a half-wave plate placed before a polarizer. Polished samples of c-cut Ti:Sapphire with a Ti^{3+} concentration of 0.5 at. % were mounted on a computer controlled XYZ motion stage (Physik Instrumente) that allows translation parallel or perpendicular to the laser propagation axis. The laser beam was focused inside the target by a long working distance 10 × Mitutoyo microscope objective (working distance 34 mm, nominal numerical aperture NA = 0.28). A longitudinal writing configuration, with translation parallel to the laser propagation axis (along the c-axis direction) was used throughout the text unless otherwise mentioned. An Olympus BX51 positive phase contrast microscope (PCM) was employed to monitor the interaction region in a side-view geometry. In this arrangement, the relative positive index changes are appearing dark on a gray background, while white zones indicate negative index variations or scattering centers. The end facets of the waveguides were ground and polished after laser irradiation. Optical near-field mode profiles were recorded with a 20 × microscope objective and a charge-coupled (CCD) camera. Waveguides were illuminated using an additional incoherent white light (WL) sources and polarized 800 nm CW light. Real-time PCM imaging and in-line near-field mode measurement make the experimental setup be a highly efficient workstation for waveguide writing.

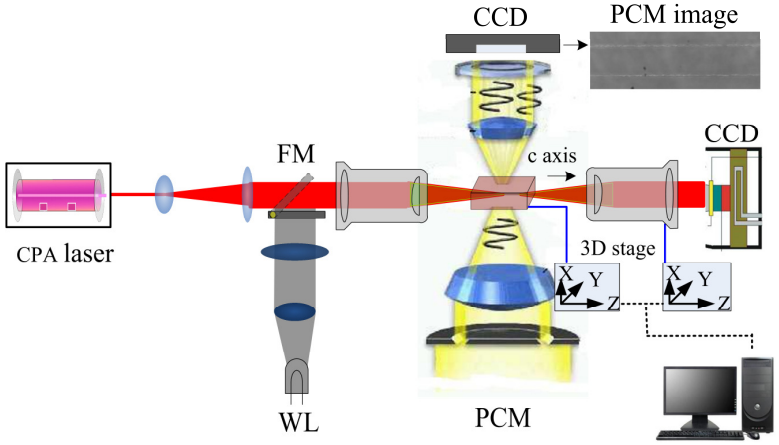

Fig. 1. Experimental setup of the femtosecond laser waveguide writing arrangement indicating the irradiation geometry and crystal orientation: FM flip mirror, CCD charge-coupled camera, PCM phase contrast microcopy, WL white light source.

The laser-induced traces were further analyzed using optical transmission (OTM) and cross-polarization microscopy (CPM) to distinguish stress birefringence. Subsequent to irradiation, the written traces were also exposed in cross-section after polishing and etching following the technique presented in [9], and imaged using Scanning Electron Microscopy (SEM).

3. Results and discussion

3.1 Photoinscription of single and parallel lines

The critical power for self focusing in sapphire crystals equals a few MWs. For sufficient irradiation exposures, above the critical power, a single line structure fabricated in the crystal

#166874 - $15.00 USD Received 17 Apr 2012; revised 25 May 2012; accepted 4 Jun 2012; published 20 Jun 2012

may produce a lower density negative refractive index change in the trace as the material may loose crystalline order and thermo-mechanically expand. A shallow positive index appears around the main traces due to possible stress [11]. As the typical modification in a single line is a dominantly negative change, the concept used for fabricating waveguides was based on stress confinement and accumulation of compaction in the stressed regions between the two neighboring lines.

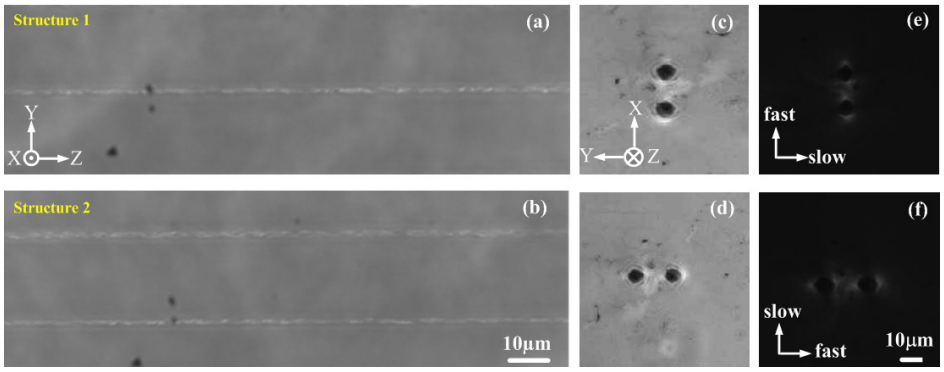

Fig. 2. Phase contrast, transmission and birefringence microscopy side/axial images of the waveguides in Ti:Sapphire crystal written by fs laser pulses. All the structures are written by horizontally polarized (parallel to Y) laser pulses at the scanning speed of 50μm/s. The length of all traces is 3 mm. (a) Top view PCM image of two waveguides written in XZ-plane (denoted structure 1). Note that due to the vertical arrangement second trace lying behind is not visible. (b) Top view PCM image of two waveguides written in YZ-plane (denoted structure 2). The distance between the double traces is 25μm. (c) and (d) End view transmission microscopy images of structure 1 and structure 2, respectively. (e) and (f) End view polarization/birefringence microscopy images of structure 1 and structure 2, respectively. White region in (e) and (f) shows strong stress-induced birefringence. Fast axis and slow axis are indicated in (e) and (f) according to the two orthogonal polarization guiding mode. The writing pulse energy was 50μJ and the pulse duration was 120fs.

To achieve this fabrication concept, the sample was held on a translation stage that moved in a direction parallel to the writing beam. Two parallel lines separated 25μm were written by translating the sample with a speed of 50 μm/s, creating a potentially guiding trace in between where light can be subsequently injected. Waveguides that are based on stress in the crystal are inherently asymmetric since they are always located next to the low index modification. Here the decreased refractive index acts as a strong barrier for the guided mode. The writing-pulse energy was 50μJ. Figure 2(a) and 2(b) show PCM images of the double tracks written in XZ plane (denoted structure 1) and YZ plane (denoted structure 2), respectively. White color trace in PCM indicates negative index changes with respect to the matrix.

3.2 Optical and birefringence imaging

The Ti:Sapphire crystal undergoes strong disorder and volume increase in the exposed region upon the irradiation with fs laser pulses [13]. At the same time, stress is induced in the surrounding material. In optical materials, glassy or crystalline, the magnitude of stresses in microstructures can lie in a large range from MPa to GPa depending on the focusing conditions [14–16]. In our case, the initial pressure leading to thermo-mechanical constraints can be roughly estimated as $P = \alpha E \Delta T$, where α is the average mechanical expansion coefficient, E is the Young modulus and ΔT is the temperature variation during the laser modification, provided that heating occurs very fast. Here α = 8.1 x 10^{-6}/ °C and E = 345 GPa. ΔT is considered around the melting point of Sapphire (2040°C). The maximum stresses in the interaction region which can amount to significant values in sapphire (about 5.7GPa) due to a large Young modulus and directionally selective high expansion coefficients, can cause the inhomogeneous and anisotropic distribution of refractive indices by the elasto-optic effect [17,18]. The correspondingly emerging stresses accumulating

#166874 - $15.00 USD Received 17 Apr 2012; revised 25 May 2012; accepted 4 Jun 2012; published 20 Jun 2012

between the double traces are slightly lower than that in the interaction regions. Using standard transmission and cross-polarization microscopy we investigated the absorbing, scattering and birefringence properties of the region in the vicinity of the double tracks. Figure 2(c) and 2(d) depicts the end view transmission microscopy images of the two structures, respectively. Dark region shows strong scattering of the disordered structure. White regions surrounding the dark traces represent guiding modes of white light due to stress birefringence and index increase. With the cross-polarization microscopy, the birefringence property of the region in the vicinity of the double tracks was equally analyzed in a qualitative manner, with a quantitative estimation given latter in the text. The birefringent character is shown in Fig. 2(e) and 2(f). Laser unexposed regions around the dark tracks and between the double photowritten lines indicate stress-induced birefringence. To be noted here, the end view of the laser-induced traces under cross-polarization microscopy is dark due to strong scattering. As it will be seen later, this is due to the formation of nanogratings that contribute to a negative phase retardation and light scattering [5] inside the trace.

3.3 Guiding modes

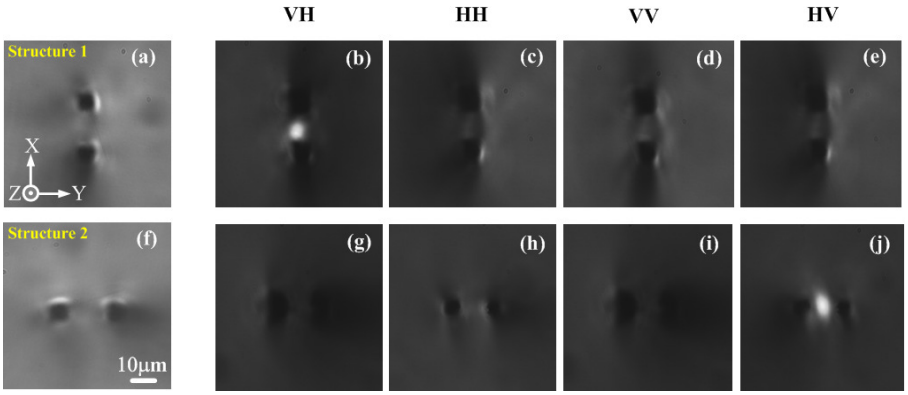

Fig. 3. Microscopy and near-field mode images of structure 1 and structure 2 for injected 800 nm radiation with two orthogonal polarization directions respectively. In the letter "AB" on the top of each column the first letter represents the writing polarization, and the second letter represents the injection polarization. (a, f) Microscopy image of the structure 1 and 2. Polarization dependent optical guiding properties in the double line structure were observed (b-e, g-j). The guiding is sensitive to structure configuration and polarizations. Horizontal polarization can be guided only in structure 1 written with vertically polarized radiation (see Fig. 3(b)); the vertical polarization can be guided in horizontally polarized written structure 2 (see Fig. 3(j)).

In order to investigate how the writing laser polarization impacts on the guiding mode, both horizontal (denoted H, electric field vector along Y axis) and vertical (denoted V, electric field vector along X axis) polarizations were adopted for photoinscribing structure 1 and structure 2. Figure 3 depicts near-field modes of guided 800 nm light injected in the core, between the lines. A noticeable polarization sensitivity of the structures was observed. Horizontal polarization can be guided in structure 1 shown in Fig. 3(b) written by vertically polarized laser pulses. No guiding modes were observed in the other cases related to the polarization of the injected light. On the other hand, only the vertical polarization can be guided in horizontally polarized written waveguide in structure 2, shown in Fig. 3(j).

A similar effect was observed in fused silica. As indicated in ref [5], the guiding rule of type II waveguide in fused silica is that the injection polarization must be orthogonal to the writing polarization. We attributed this polarization sensitive guiding in fused silica to nanogratings induced by linearly polarization laser. In anticipation of the nanostructures observed previously in sapphire [9], we investigate their presence in the bulk by checking the cross section of the trace in Ti:Sapphire.

#166874 - $15.00 USD Received 17 Apr 2012; revised 25 May 2012; accepted 4 Jun 2012; published 20 Jun 2012

3.4 Nanogratings generation

Figure 4 shows the SEM images of the cross section of the traces written with vertically and horizontally polarized ultrashort laser pulses. After lapping and polishing the end face of the track, the crystal was etched for 5 minutes in 10% aqueous solution of HF acid. The modified regions obtained a significant change in the exposed surface morphology required for subsequent investigating with SEM. The average period of self-organized nanostructure grating is about 230 nm. The nanoplane is orthogonal to the polarization of the writing beam.

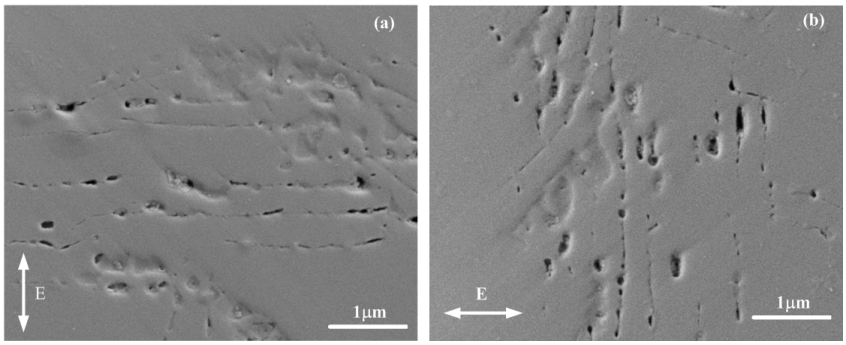

Fig. 4. SEM images of the cross section profile of a single line trace produced by the 120 fs, 800 nm, 50μJ pulses in sapphire after etching for 5 min in 10% aqueous solution of hydrofluoric acid. (a) is written by vertically and (b) is written by horizontally polarized ultrashort laser pulses.

Nanogratings formation is often associated with collective electronic oscillations of denser laser-induced electron plasmas. Couairon suggested already a particular structural damage associated with an electron-ion plasma triggered by avalanche [19], moving away from the regime of intensity clamping and the associated leveling of electronic density [8]. This regime is sensitive to the initial seed electrons produced by multiphoton ionization determining carrier multiplication, and therefore to pulse duration, but equally to spatial inhomogeneities.

The hypothesis of transient nanoplasmonics can assist in understanding the nanograting formation. This suggests how the nanoplanes are first assembled from smaller structures and then subsequently self-ordered on a long-range scale [20]. However, according to the nanoplasmonics scenario, nanograting formation should not be very sensitive to the interaction media with the exception of the number of initiation centers. Until now, uniform nanogratings was already observed in fused silica, doped silica glass [21], TeO_2 crystal [22] and sapphire crystal, but were not identified in borosilicate BK7, doped phosphate glass, tellurite oxides, and $LiNbO_3$, where apparently the cohesion energy of the bonding strength plays a role [23]. In most cases, the period of nanogratings is several hundred nanometers. This suggests that melting on large regions should not happen during the nanograting formation, merely a viscosity decrease assisting the material hydrodynamic movement via cavitation in soft phases. So short pulse duration and high melting point of media are necessary. The previous experiment shows that the domain of nanogratings increase slowly with the augmentation of the pulse duration [8].

3.5. Light transport properties

Firstly, the nanostructures formed in the trace can be considered responsible for this polarization dependent guiding phenomenon, acting as a birefringent cladding with a scattering efficiency which is polarization dependent. Maximal transmission for the injected light occurs when the electric vector is parallel to the nanoplane and maximum scattering or mode leaking occurs when light vectors are perpendicular to the nanoplanes. Consequently the guides allow light transport for polarizations aligned along the planes and scatter radiation for polarizations aligned orthogonal to the planes. According to this, as in the case of type II waveguide in fused silica, it is understood that guiding of the mode occurs in Fig. 3(b) and

#166874 - $15.00 USD Received 17 Apr 2012; revised 25 May 2012; accepted 4 Jun 2012; published 20 Jun 2012

3(j) and no guiding mode appears in the Fig. 3(c), 3(d), 3(h) and 3(i). To be noted here, Fig. 3(e) and 3(g) are out of the rule. We have therefore to consider an additional mechanism. As shown for $LiNbO_3$ [11], this can be attributed to and additional structure sensitive guiding property which originates from the stress-induced birefringence.

Secondly, stress-induced birefringence induced by fs laser pulses in the crystal results in an anisotropic distribution of the refractive index [12,24]. The direct laser writing method involving tightly focused fs laser pulses was used here to fabricate regions of amorphous sapphire inside the original crystalline sample at similar conditions as in the previous studies [25,26]. Cracks can be observed under optical microscopy or nanocrack under SEM. Polariscopy and phase imaging is used to quantify the stress-induced birefringence. The laser-generated stress-birefringence between the double laser traces amounts up to 10^{-3} for visible wavelengths, (consistent with the GPa stress magnitudes [15] originating from thermal expansion indicated before) and the stress volumes span on tens of microns. Due to stress birefringence, light confinement between the two tracks is totally different for horizontal and vertical configurations. Between the double tracks induced by laser irradiation in structure 1, the index change is positive for horizontal and negative for vertical polarization. We mention that a similar behavior was reported in crystals. The observed behavior in the core is similar as the one involved in writing waveguides in $LiNbO_3$ crystal written by fs pulse, and other stress induced waveguides [11], and fabrication in Ti:Sapphire may carry interest due to higher resistance to damage and heat.

In view of the above-mentioned facts, the polarization dependent guiding in Ti:Sapphire can be explained by a mix of two polarization-sensitive mechanisms: polarization dependent scattering of the nanostructures combined with a birefringent structure core index change which is equally polarization sensitive. The total loss of the double line structures was measured by end coupling a 980nm diode laser (outside the absorption band of the Ti:Sapphire) into the structure. A single mode fiber and a short-focus aspheric lens were used to couple and collect the light. The total loss of the 3mm-long waveguide was 1.1dB for guiding mode. In consideration of inevitable coupling loss between waveguide and fiber, the propagation loss should be less than 3.67dB/cm. Typical propagation loss for fs-written waveguide in the $LiNbO_3$ crystal is around 1dB/cm, suggesting a similar range of losses in our case and the 2.5dB/cm propagation loss value mentioned in ref [10]. In addition, the extinction ratio of the double line structures depends on the length of the waveguide. The extinction ratio can be improved when longer waveguide length is adopted. The further use of the polarization dependent guiding property for the fabrication of high extinction ratio channel waveguides polarizer in Ti:Sapphire could be highly advantageous in integrated optical circuits, particularly for light transport and potential amplification.

3.6. Complex structures

In order to investigate the guiding of 3D assembling of traces, two 3 × 3 waveguide arrays were fabricated with vertically and horizontally polarized laser pulses respectively. The distance between the neighboring traces is 25μm. The length of all traces is 3 mm. We injected 800nm laser at the center of each two neighboring traces in turn. Figure 5(a) and 5(c) depict near-field mode images of the waveguide array injected with horizontal and vertical polarizations respectively. All the guiding modes positions were shown by red spots in Fig. 5(b) and 5(d). The results support the previous conclusion extracted from the polarization dependent double line structure. However modes coupling is not apparent in this case, a large distance between two possible modes and effective normalized waveguide frequency may play an important role to diminish the mode coupling.

#166874 - $15.00 USD Received 17 Apr 2012; revised 25 May 2012; accepted 4 Jun 2012; published 20 Jun 2012

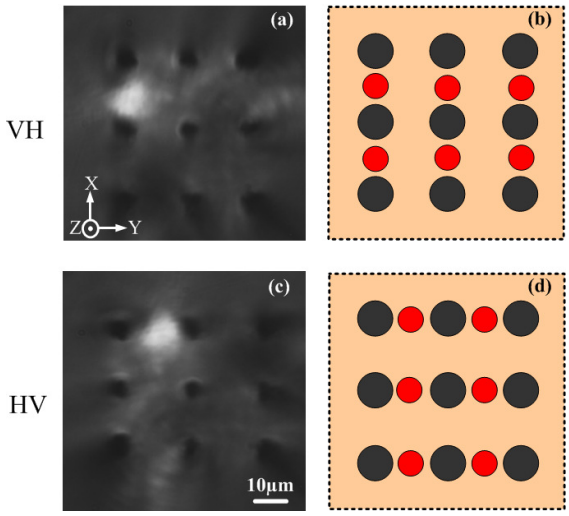

Fig. 5. Near-field mode images of 3 × 3 waveguide array. Two orthogonal polarizations of 800 nm radiation were injected at the center of each two neighboring traces, respectively. The letters on the left column indicate the polarization of the writing and injection laser. The red spots in the structure represent the guiding positions.

In a previous paper [5,8], we have reported that diamond, hexagon and octagon structures consisting of type II traces lead to particular polarization dependent light transport properties due to form birefringence in nanogratings determining a low index cladding of the waveguide. That kind of 3D structure shows the ability of guiding light in fused silica related to the orientation of the nanostructures. Here we equally investigate a diamond structure as shown in the left part of Fig. 6. In Fig. 6(a) top and bottom traces were written by vertical polarization, and left and right traces were produced by horizontal polarization. So Fig. 6(a) consists from the superposition of the structures depicted in Fig. 3(b) and Fig. 3(j) where each individual arrangement can guide light. However, the global structure is not able to guide light. We attribute this to orthogonal nanograting which scattering all the polarizations of the injected light.

Also a hexagon structure was written by horizontally and vertically polarized laser pulses respectively. The end face picture under transmission optical microscope presents a grey guiding region shown in Fig. 6(b), however no guiding mode was observed under any polarization of the laser injection. This is a behavior different from the case in fused silica, which permits the guiding of light perpendicular to the structures. In particular, a hexagon structure written by the horizontal polarization of the laser in fused silica guides horizontally polarized light (see Fig. 6(e)). There are two effects concurring to achieve this behavior. First of all, polarization dependent scattering of nanogratings can extinguish one polarization. Secondly, stress-related region of the birefringence induced by fs laser expands typically in the range of 24 μm around the damaged trace in sapphire crystal [15]. The six spots are separated by 25 μm from each other and the effective index in the middle of hexagon is prone to no change. That is why hexagon structure in sapphire cannot guide

#166874 - $15.00 USD Received 17 Apr 2012; revised 25 May 2012; accepted 4 Jun 2012; published 20 Jun 2012

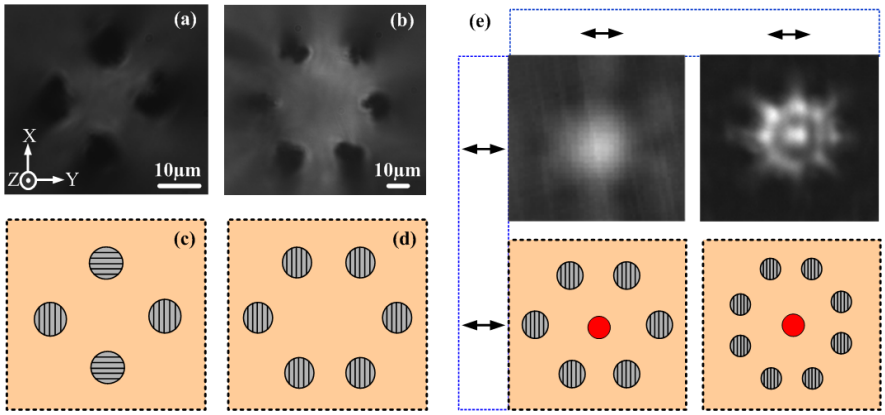

Fig. 6. Near field mode images of the cross-sections of diamond structure (a) and hexagon structure (b) written by ultrashort laser pulses with horizontal and vertical polarization respectively. Two orthogonal polarizations were injected into the center of every structure respectively, but no guiding modes were observed for 800nm injected radiation. (c) and (d) show the orientation of the nanogratings in the rods of the diamond diamond, respectively the hexagon structure. The length of all traces is 3 mm. (e) shows the particular polarization dependent light guiding properties of the hexagon and octagon structures in fused silica [3,6], The red spots in the structure represent the guiding positions, the arrows on the left column indicate the polarization of the writing laser, the arrows on the top of each column indicate the polarization of the injection laser.

4. Conclusion

In conclusion, we have observed polarization sensitive guiding properties of double line structures in sapphire. The polarization dependent guiding can be explained by the birefringent stressed core combined with polarization dependent scattering of the surrounding nanostructures. The subwavelength pattern located inside the marginal traces develops perpendicular to the laser polarization as confirmed by electron microscopy inspection. Based on the observed polarization sensitive characteristics and on the double-line concept, 3 × 3 waveguide arrays were realized in the crystal with the same polarization sensitive behavior, without apparent mode coupling. Complex 3D diamond and hexagon were equally investigated and the role of birefringence was discussed in comparison to fused silica. Thus, relying on guiding and polarization functions, the fabricated structures emerge as promising candidates for the future development of integrated optics elements in the Ti:Sapphire or sapphire crystals.

Acknowledgments

This work was supported by West Light Foundation of The Chinese Academy of Sciences (No.0729591213) and Innovative Research International Partnership Project of The Chinese Academy of Sciences.

#166874 - $15.00 USD Received 17 Apr 2012; revised 25 May 2012; accepted 4 Jun 2012; published 20 Jun 2012